Self-organized collective escape in bird flocks

Papadopoulou, Marina

DOI:
10.33612/diss.255711610

Chapter 4.

Collective turning in bird flocks: predator confusion by self-organization

~ M. Papadopoulou, H. Hildenbrandt, & C.K. Hemelrijk ~

Abstract

The main driver of the evolution of animal aggregation is protection against predators. During their collective escape, bird flocks confuse the predator by rapid changes in their shape and internal structure. The confusion of the predator results from many prey passing through its field of view, challenging its targeting of a single individual. Little is known about how the specifics of collective escape affect the confusion of the predator, even for the most common pattern of collective escape, the collective turn. To gain this understanding, we developed a computational model (agent-based), in which flocks turn towards their roost or away from an attacking predator, similar to real flocks. To examine whether turns with 'equal-radii' confuse the predator more than turns with 'parallel-paths', as previously assumed, we developed a new metric of deviation from these two types of turning. As a proxy of predator confusion, we used the instability of neighbors: the rate with which the closest neighbors of a flock member are changing. In our simulations, we investigated how flock size, ecological context (roosting or evading), turning rate, and specifics of coordination (topological range, strength of alignment and attraction, and reaction frequency) affect the instability of neighbors, as well as its relation with the two turning types. Across our parameter space, we show many counter-intuitive effects of flock characteristics and coordination on the instability of neighbors, as well as unexpected relations between neighbor instability and the deviation from equal-radii and parallel paths, highlighting the complexity of collective turning. Our study provides a framework for investigating collective turning across species, supporting research on collective navigation, escape, and swarm robotics.

4.1 Introduction

The primary advantage that grouping offers to animals in nature is protection against predators [34]. This advantage is rooted in the potential earlier detection of predators (many-eyes hypothesis [111]), the decrease in the probability of a single individual to get caught instead of its group mates (selfish-herd hypothesis [61]), and the decrease in the hunting success of the predator due to many prey individuals passing through its field of view (confusion effect) [34, 105, 83]. In bird flocks, a predator's confusion has been linked to the diffusion of the flock, with how quickly group members change their relative positions, reshuffle in the field of view of the predator and change their interaction network (neighbor stability) [27]. Neighbor stability has, however, only been studied in large flocks of starlings during collective turning above a roost [27].

Collective turns are a major method by which flocks of birds respond to predators [165, 131]. It is observed in many bird species that form flocks with different characteristics, from small groups of crows and homing pigeons to large flocks of jackdaws and starlings, and across many ecological contexts, while a flock is foraging (returning home) [115], roosting (circling around roost) [10, 185], and actively trying to evade a predator [131]. Even though the propagation of turning in bird flocks has gained the attention of researchers almost 100 years ago [159], the complexity of collective turning has only recently been recognized [115].

Pomeroy and Heppner (1992) [142] were among the first that analyzed collective turns in birds. By studying the turning patterns of small flocks of pigeons, they noted that all flock members move along an arc of a similar radius and their paths cross during a collective turn [142]. Such collective turns are referred to as 'equal radii' (Figure 4.1) and have also been observed in starling flocks [10, 8].
In contrast to this turning type, individuals may differ in their turning radii and maintain their relative positions through a turn (Figure 4.1). In this case, group members turn without crossing their paths, a so called "parallel-paths" turn [142, 185], resulting in a flock with a stable shape and internal structure [10]. Even though turns with parallel-paths have been assumed to be unlikely in bird flocks [10, 8], they have partly been observed in pigeons flying above their roosting site [185]. In reality, a flock's turn is probably in between the two turning modes [185].

The characteristics of a flock during a collective turn have been studied in large flocks of starlings based on a series of measurements [10, 27, 8, 72]. First, the rate of change in the social network of a group during a turn is captured by the amount of time in which the set of closest neighbors of each group member changes (referred to as 'stability of neighbors') [27]. Secondly, two measurements of a flock's diffusion capture changes in the group's internal structure

based on the degree of individual displacement relative to the position of its neighbors ('mutual diffusion') and the flock's center ('global diffusion') [27, 72]. Based on these measurements, it has been found that flocking starlings change all their nearest neighbor every few seconds during collective turns while flying above their roost [27]. High diffusion and low neighbor stability, apart from influencing the propagation of social information in a group, have also been linked to increased predator confusion [27]. Our knowledge about the emergence of these properties (high diffusion and low neighbor stability) across species and their relation with different turning modes is unfortunately still limited.

According to the principles of self-organization, collective properties such as flock shape and diffusion (global and mutual) emerge from group members coordinating their motion through simple interactions with neighbors nearby [72]. The specifics of these local interactions (referred to as 'coordination') differ across species and ecological contexts. For instance, each individual may interact by aligning its heading with a certain number of closest neighbors (referred to as 'topological range'), moving towards these neighbors to stay with the flock or away from them to avoid collisions [9, 81]. For starlings, when circling around their roost, the number of interacting neighbors is 6-7 [9], while jackdaws in foraging flights coordinate more with their mating partners and 3 other closest neighbors [112]. During mobbing, jackdaws interact with all neighbors within a given radius instead (referred to as 'metric' interactions) [114]. Metric interactions have also been found in flocks of swifts [45]. When under threat, prey individuals may further change their behavior, for instance by increasing their reaction frequency [41, 79]. The link between the specifics of these rules of motion and coordination and the pattern of collective turning is currently lacking.

In the present chapter we aim to study collective turns in detail theoretically, in order to understand how the specifics of coordination in bird flocks affect the confusion of their aerial predators. As a proxy for predator confusion, we use the reshuffling of flock members while collectively turning (neighbor instability) [27]. We develop a biologically inspired computational model of collective motion and simulate collective turns that resemble roosting (turning around a stable and global point in space) and evasive (escape maneuver) behavior we see in nature [10, 8, 185, 125]. A turn in our model is initiated by one (or a few) individuals and propagates through the group, as in real flocks [115].

We test a series of hypotheses based on self-organization [24]. We hypothesize that neighbor instability increases when individuals interact with fewer nearby neighbors (H1) and less often (H2) and with weaker alignment interactions (H3) and stronger centroid attraction (H4, since individuals will turn more and thus reshuffle more). We further expect instability of neighbors to be higher in roosting turns than evasive turns (H5), given that the local conditions of each flock member (relative position) differ when they are attracted to a spe-

cific (global) location of a roost rather than evading a close-by predator. Since former studies on the two different modes of collective turning (equal-radii or parallel-paths) are limited [142, 185, 8], we also examine how neighbor instability relates to these types. To detect the type of collective turning, we develop a metric inspired by mutual diffusion: an estimate of the deviation of individual trajectories from each type of collective turning. We expect neighbor instability to be higher in collective turns with low deviation from equal radii (H6) and high deviation from parallel-paths (H7).

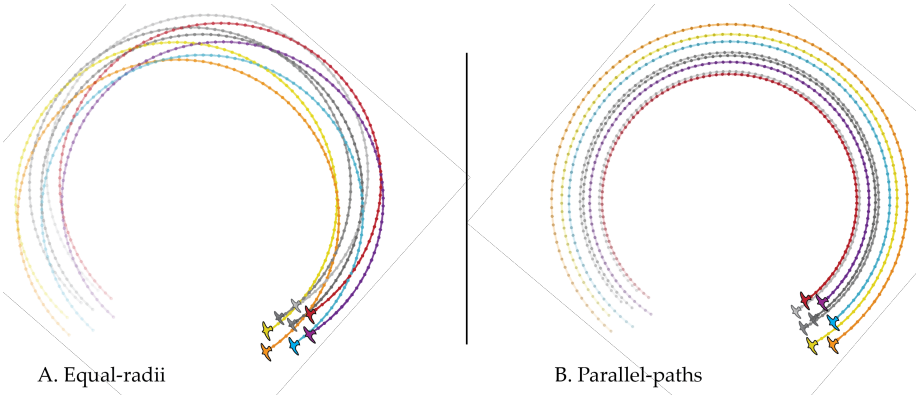

Figure 4.1: **Type of collective turn** A. Equal-radii: individuals perform a turn of identical radius and thus change their relative positions. B. Parallel-paths: individuals keep their relative positions the same by performing turns of different radii (varying their angular velocity).

4.2 *ColT*: a model for collective turning

We built an agent-based model of collective motion (flocking) named *ColT* (Collective Turning), in which individuals perform collective turns in a large 2D space. We developed the model in 2-dimensions since collective turns in real flocks mostly lie on a plane [185, 27]. Our model is based on the principles of self-organization: local interactions among neighboring bird-agents lead to emergent patterns of flocking. Collective turns emerge from the individual tendency to turn while coordinating. We model this tendency as a steering vector with magnitude controlled by a turning-weight parameter. Between events of collective turning, the flocks move forwards (straight flight). In the model, time is measured in seconds, distance in meters, and angles in degrees.

4.2.1 Collective motion

Each agent is defined in the global coordinate system by its position ($\vec{r}_i$) and its velocity ($\vec{v}_i$). The unit vector of an agent's velocity (heading vector $\hat{h}_i$) defines the local coordinate system of the agent through which it senses its neighbors. Agents have a preferred speed from which they deviate to catch up or avoid collisions with their neighbors. To reflect the inability of individuals to infinitely increase their speed, our agents are dragged back to their preferred speed based on the same drag force used in the HoPE model (Chapter 2 and 3, Eq. **(2.1)**).

Agents coordinate according to the rules of alignment, attraction and avoidance with the surrounding individuals (referred to as 'neighbors', N_i) that are within their field of view (FoV). An agent aligns with the average heading of its n^{topo} closest neighbors and turns towards their center of mass. The strength of this attraction depends on the distance of the individual to the center of its neighborhood: the further away it is, the more it is attracted towards it. To avoid collisions, an agent turns away from the position of its closest neighbor [72] in a range of minimum separation (d_{sep}). Let $\vec{s_{ij}} \equiv \vec{r}_j - \vec{r}_i$ be the position of neighbor j in the reference frame of a focal individual i at a given time point. Thus, the steering vector ($\vec{\alpha}_{social}$) that controls the motion of each individual is the weighted sum of these coordination rules:

$$\vec{\alpha}_i^{social} = w_a \frac{\sum_{j \in N_i} \hat{h}_j}{n^{topo}} + w_c \gamma_c \frac{\sum_{j \in N_i} \vec{s_{ji}}}{|\sum_{j \in N_i} \vec{s_{ji}}|} + w_s \beta_s \frac{\vec{s_{j_1 i}}}{|\vec{s_{j_1 i}}|} + \epsilon_i \hat{h}_i^{\perp} \tag{4.1}$$

where N_i is the neighbor set of focal individual i (with cardinality n^{topo}), $\hat{h}_j$ is the heading vector of a neighbor j, $\vec{s_{j_1 i}}$ is the position of i relative to its closest neighbor (j_1), ϵ_i is a noise scalar sampled from a uniform distribution based on the parameter β_w, and $\hat{h}_i^{\perp}$ is the unit vector perpendicular to the heading vector of i. The w parameters (w_a, w_c, and w_s) represent the weights of alignment, centroid attraction, and separation, respectively, that control the influence of each 'rule' at an individual's motion. As in HoPE (Chapters 2 and 3), we model asynchronous interactions: each agent updates its information about its neighbors' position and heading with a constant frequency (f_r) but not necessarily at the same point in time as its neighbors.

4.2.2 Collective turning

In $ColT$, turns are randomly initiated by one (or rarely a few) individuals. We label this agent as 'the initiator'. Each agent has a probability of becoming an initiator by entering a 'turning' state. The neighbors of an initiator may copy its turning behavior, resulting in the turn propagating through the flock (Figure 4.2A). We model two different contexts of collective turning when under attack by a predator: 'roosting', in which individuals are attracted towards a

global point in space (inspired by starling flocks circling above their roost in the presence of a predator [8]), and 'evading', in which they perform a turn of predefined angular velocity away from a predator (evasive turn, inspired by pigeon flocks reacting to an artificial predator, the RobotFalcon [156], Chapters 2 and 3). While turning, individuals keep coordinating with each other as described above.

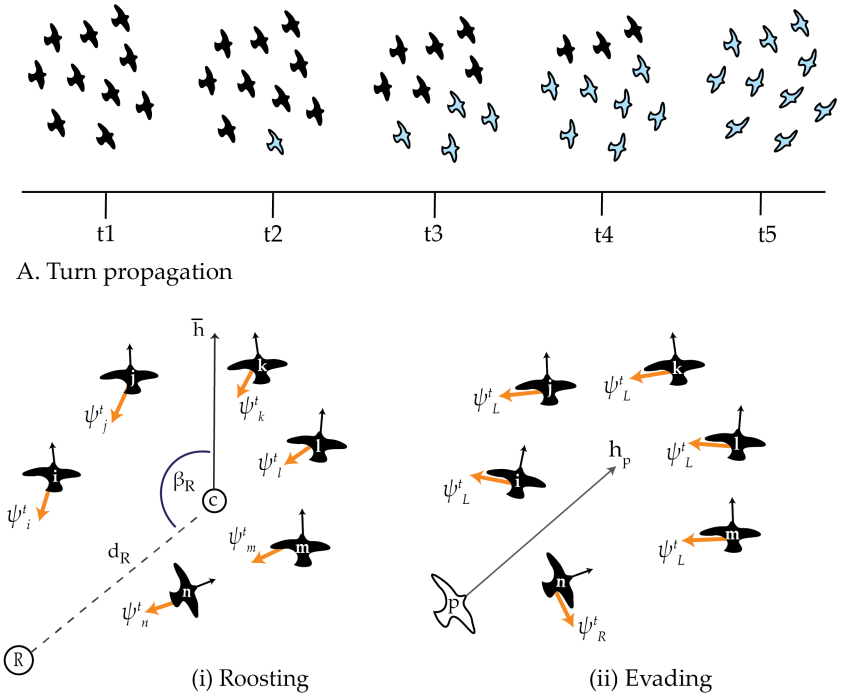

Figure 4.2: **Turning in the model *ColT*.** A. Schematic of how a turn propagates from a single initiator to the rest of the flock through individuals copying the behavior of their neighbors. Light individuals represent group members that are turning. B. The specifics of the two types of turning rules in the model. Orange arrows ($\vec{\psi}^t$) represent the steering vectors that make individuals turn. In roosting (Bi), individuals are attracted to a roost (R), defined by a distance from the flock's center (d_R) and an angle (β_R) relative to the flock's heading (average heading of all flock members), $\bar{h}$. Since the roost is a global point in space, each group member has a different relative position to it (different local conditions) and thus the tendency of each individual to turn differs. During evasive turns (Bii), individuals are turning away from the predator's heading ($\hat{h}_p$) from a constant steering-vector that is perpendicular to the left ($\vec{\psi}^t_L$) or to the right ($\vec{\psi}^t_R$) of each individual's heading. Thus, when the flock turns collectively, all flock members have the same tendency to turn (their steering vectors to evade the predator have the same constant magnitude).

We make agents turn by applying an extra steering vector ($\vec{\psi}^t$) for a specific amount of time. The specifics of turning differ between the two ecological contexts that we model. For roosting, we add a vector with direction from the focal's individual position towards a point in space that represents the flock's roost. This point is calculated at the beginning of every turn at a given distance (d_{roost}) and angle (β_{roost}) away from the center of the flock (Figure 4.2Bi). The magnitude of this steering vector (and thus influence on the agent's motion) is controlled by the parameter w_t. For evasive turns, we add a steering vector perpendicular to each individual's heading. In this case, the vector points to the direction away from the heading of the predator (Figure 4.2Bii). For this, we model a dummy predator-agent that follows the flock from behind (from a given distance and bearing angle, as in the HoPE model [131]). The strength of the force is such that individuals perform a turn with a predefined angular velocity (e.g., 90°, parameter β_{esc}, within a given turning time, t_{esc}).

We give each flock member a unique probability to start turning, similar to performing an escape maneuver in the HoPE model (Chapters 2 and 3). If the neighbor of a focal individual is roosting or evading, the steering vector for turning towards the roost or away form the predator, respectively, of the focal individual is activated (it 'copies' its neighbor's behavior). We give turns a predefined duration at the level of the individual (t_{turn}). The total steering force of every agent is thus calculated by:

$$\vec{\alpha}_i^{steering} = \vec{\alpha}_i^{social} + w_t \vec{\psi}_i^t \qquad \text{Steering vector} \qquad (4.2)$$

We use $\vec{\alpha}^{steering}$ to update the position and velocity of each agent at each time step ('integration' time step, dt) as we do in the HoPE model (see ODD protocol of Chapter 3, section 3.B, and Eqs. (3.30)-(3.33)).

4.3 Methods

4.3.1 Neighbor instability

To study the confusion of the predator, we analyzed the time-series of the position and heading of each flock-member during collective turns in our simulations. The periods of free flight were discarded. We use changes in the flock's internal structure as a proxy of predator confusion by calculating an established measurement of diffusion over a sliding time-window: 'neighbor stability' [27, 72]. This measurement (previously also referred to as 'neighbor overlap' [27]) captures the rate with which individuals change their network of interacting neighbors while changing positions in relation to the flock's center ('global diffusion') and each other ('mutual diffusion') [27]. Since here we focus on predator confusion that is expected to increase with decreasing neighbor stability, we analyze our results looking into the 'instability of neighbors'. In detail, instability of neighbors (Q_M) is estimated by measuring how much the set of closest M neighbors of a focal individual $M_i(t)$ changes over time:

$$Q_M(t) = 1 - \frac{1}{T-t}\frac{1}{N}\sum_{t_0=0}^{T-t-1}\sum_{i=1}^{N}\frac{|M_i(t_0)\cap M_i(t_0+t)|}{M} \tag{4.3}$$

where N is the number of flock members, T the total length of our measuring window, $M_i(t_0)\cap M_i(t_0+t)$ the intersection of the closest neighbors of individual i at time t_0 and t. We average over all individuals in the flock and all initial time points t_0. Based on (4.3), neighbor instability ranges from 0 (if all neighbors are the same) to 1 (if all neighbors have changed over the given time period). To examine how neighbor instability varies through our parameter space, we also note the ending value from each instability time-series (at the end of our sliding window t_w).

4.3.2 Measuring collective turns

To measure how close a collective turn resembles one of the two turning modes, equal-radii and parallel-paths, we created measurement inspired by mutual diffusion [27]. Our measurement estimates how much the flock members' trajectories during each collective turn deviate from each type based on the expected position of neighbors if a turn with parallel-paths or equal-radii has taken place (Figure 4.1). Let $\vec{s_{ij}} \equiv \vec{r_j} - \vec{r_i}$ be the position of neighbor j in the reference frame of a focal individual i at a given time point, and $\vec{s'_{ij}}$ its position at the consecutive sampling point during which the focal individual turned by θ degrees. For equal-radii turns, we expect that:

$$\vec{s'_{ij}} == \mathbf{R}(-\theta_i)\cdot\vec{s}_{ij} \tag{4.4}$$

where R is a rotation matrix, reflecting that j has moved in the opposite direction of i's turn by θ_i^o. For parallel-paths, the relative position of individuals remains the same, thus we expect that:

$$\vec{s'_{ij}} == \vec{s}_{ij} \tag{4.5}$$

Based on these expected positions, let d_{dev} be the distance between the actual relative position of each neighbor at a given time and the expected position according to parallel-paths and equal-radii such that:

$$d^e_{ij}(t_1) = \frac{|\vec{s}_{ij}(t_1) - \mathbf{R}(-\theta_i(t_1))\cdot\vec{s}_{ij}(t_0)|}{t_1 - t_0} \quad \text{and} \quad d^p_{ij}(t_1) = \frac{|\vec{s}_{ij}(t_1) - \vec{s}_{ij}(t_0)|}{t_1 - t_0} \tag{4.6}$$

capture the deviation from each turning mode, equal-radii and parallel-paths, respectively, between time points t_0 and t_1. To test how these deviations scale with time, we use a sliding window (t_w) and estimate the increase of these deviations during collective turns (with T^t being the duration of a turn). We calculate the average value of deviation from a parallel-paths (D^p_M) and an equal-radii (D^e_M) turn over all flock-members in a simulation, taking into account the M closest neighbors of each individual, according to:

$$D_M(t) = \frac{1}{T^t - t_w} \frac{1}{M} \sum_{t_0=0}^{T^t - t_w} \sum_{i=1}^{M} d_{ij}^x(t_0 + t) \tag{4.7}$$

where d_{ij}^x represents d_{ij}^e or d_{ij}^p. We then average $D_M(t)$ over all collective turns in our simulations. Since neighbors' ranks change during the turn, set M contains the M closest neighbors at the beginning of every sliding window.

4.3.3 Simulations, Parameterization, & Experiments

We simulate flocks of 10, 30 and 50 individuals performing 'roosting' or 'evasive' turns for 4 to 5 seconds (T^t). The flock size and the duration and turning rate of each turn are based on empirical data of turning by flocks of pigeons and jackdaws [185, 115]. During roosting, the turning rate is represented by different tendencies to turn (controlled by the weight of the turning steering vector, w_t) and during evading by a set turning angles (θ_t). We examined low, medium, and high turning rates for each context: weighting factors of 2, 4 and 6 for roosting, and turning angles of 90^o, 135^o, and 180^o for evading. We calculated the instability of neighbors (based on the 4 closest neighbors), and the deviation from equal-radii and parallel-paths (for up to 4 closest neighbors) using a sliding window of 3 seconds (t_w).

Between turning events, flocks are performing straight flight for 15 seconds. During this time period, the flocks get back to a stable state. Each simulation lasts for 2.5 minutes and thus includes 8 collective turns. We sample data with a frequency of 0.1 seconds. Agents are initialized in a flock formation: positioned within a given radius with similar headings and speeds. The first 3 turns of each simulation are discarded to ensure that there is no effect of our initial conditions. We also discard turns during which a flock splits. After inspecting the time series of instability of neighbors and deviation from turning modes for the first 4 closest neighbors, we use for our analysis the average of the 4 neighbors for instability ($Q_4(t)$) (as previous studies on starling flocks [27, 72]) and the average deviations based on the closest neighbor ($D_1^p(t)$ and $D_1^e(t)$) of each flock member across all turns in each simulation.

Motivated by differences in coordination across species [114, 112, 45, 9, 156] and changes in the prey's behavior when under threat (namely increased reaction frequency [41, 79], increased cohesion [61, 99, 156] and switch to metric interactions [114]), we examined how the coordination specifics affect the characteristics of a collective turn. We specifically studied the effects of (1) the strength of alignment and centroid-attraction, (2) the number of interacting neighbors (topological range), and (3) the reaction frequency (how often each agent updates its information concerning its neighbors' positions). We selected the range of our parameter space after ensuring that a cohesive flock emerges. We ran 20 simulations (replicates) for each combination of parameters, ending up with 100 collective turns per parameter combination. We ran simulations

varying each parameter of interest separately, using default values for the others from the middle of each range. For a list of our parameter values see Table 4.1.

Table 4.1: **Parameters of the *ColT* model** and the values used in our simulations.

Parameter	Name - Description	Default value	Range
N	Flock size	-	$10-50$
u	Cruise speed	6 m/s	-
f_r	Reaction frequency	20 s^{-1}	$10-50$ s^{-1}
w_u	Weighting factor to return to cruise speed	0.3	-
θ_{FoV}	Field of view	270°	-
n_{ali}^{topo}	Topological range of alignment	7	$3-10$
n_{sep}^{topo}	Topological range of avoidance	1	
n_{coh}^{topo}	Topological range of attraction	7	$3-10$
w_a	Weighting factor of alignment	5	$2-10$
w_c	Weighting factor of centroid attraction	0.5	$0.2-1$
w_s	Weighting factor of separation	-1	-
w_t	Weighting factor of roosting turns	5	$2-10$
d_r	Distance to roost	20 m	-
θ_r	Angle to roost	90°	-
θ_t	Angle for evasive turns		90°-180°
d_s	Minimum separation distance	1 m	-
u_{min}	Minimum speed	3 m/s	
u_{max}	Maximum speed	25 m/s	
β_w	Range of uniform distribution of the weighting factor of the random-error force	0.2	-
Simulation			
dt	Integration time step	0.005 s	
f_s	Sampling frequency	10 s^{-1}	

4.4 Results

Examples of tracks from our simulations are given in Figure 4.3. During roosting, all individuals in our model are attracted to the same point that represents their roost (Figure 4.2Bi). In evasive turns, all individuals have the same turning rate (a vector of identical magnitude perpendicular to their headings) away from the predator, either to the left or to the right, depending on the predator's heading relative to each individual's heading (Figure 4.2Bii). The tendency to turn propagated through the group after one or a few individuals started turning (Figure 4.2A).

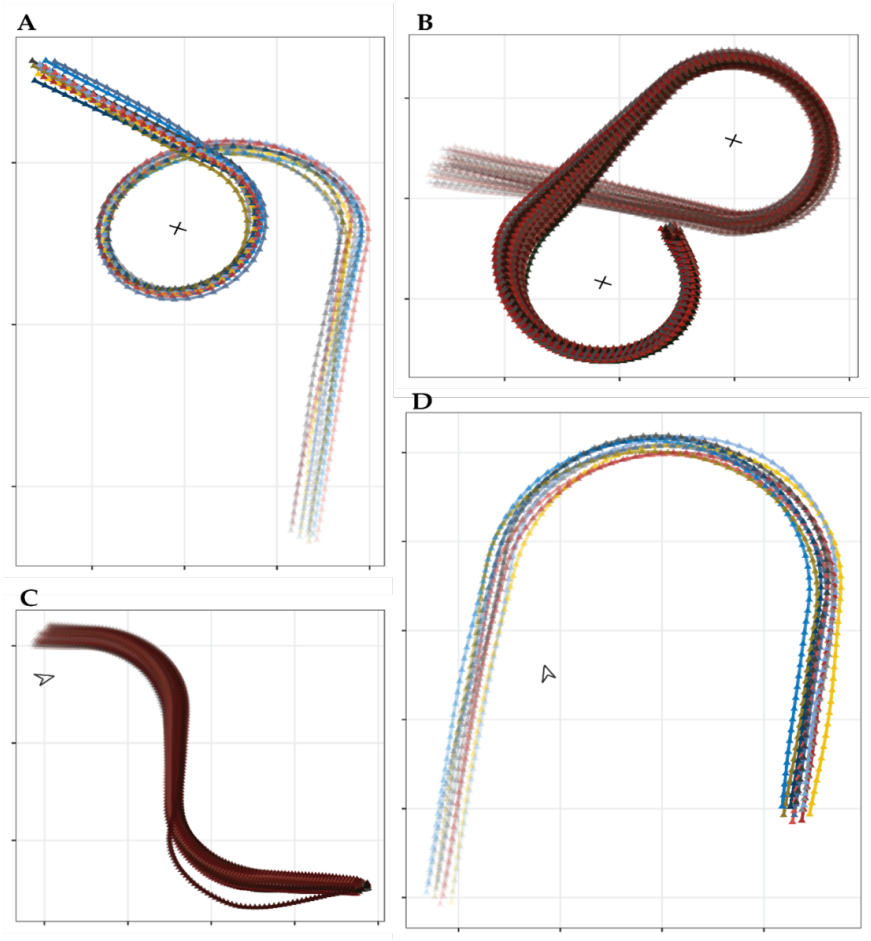

Figure 4.3: **Collective turns in *ColT*.** Simulated tracks of individuals during collective turns in flocks of different size (10 in A & D, 30 in B, and 50 in C) during roosting turns (A & B, around a global point noted by a cross) or evasive turns (C & D, away from a predator noted by a large arrow figure). Flock members may have low (A & C) or high turning rates (B & D).

4.4.1 Instability of neighbors

The instability of neighbors in our model increased over time (Figure 4.4) in a similar way as has been found in real starling flocks [27] and a previous computational model of collective motion of starlings (StarDisplay) [81, 72], with individuals losing on average 30% to 50% of their neighbors after 3 seconds of turning (Figure 4.4A). Turns with very high ($max(Q_4(3s)) = 0.85$) and very low neighbor instability ($min(Q_4(3s)) = 0.08$) emerged across our parameter space with no significant difference between evasive and roosting turns ($p-value = 0.7$,

ANOVA) (Figure 4.4A).

However, higher turning rates during roosting (as a result of stronger tendency to turn towards the roost) led to significantly higher instability of neighbors ($p-value < 0.001$, ANOVA; Figure 4.4C). This is because the turning tendencies of individuals differ while roosting, depending on each member's relative position to the roost (attraction point). As a result, at higher turning rates the effect of these small differences increased, causing individuals to reshuffle more. In evasive turns, the turning rate did not affect neighbor instability (Figure 4.4B) because individuals had identical rates (tendencies to turn) ($p-value = 0.88$, ANOVA).

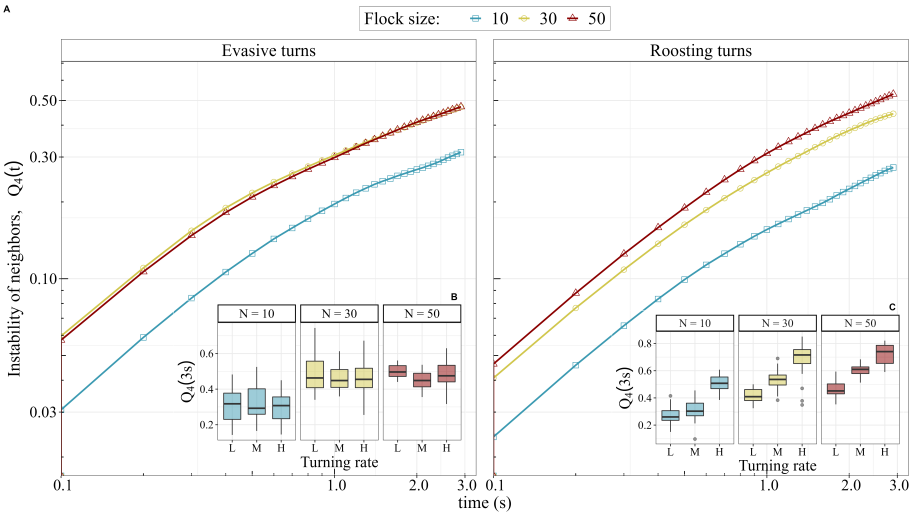

Figure 4.4: **Instability of neighbors.** A. Instability of 4 closest neighbors in evasive and roosting turns over time. B-C. Instability of neighbors after 3 seconds of turning in (B) evasive and (C) roosting turns for low (L), medium (M) and high (H) turning rates. In evasive turns, low, medium and high turning rates represent turns of 90^o, 130^o, and 180^o, while in roosting turns they represent turning tendencies of 2, 5, and 10, respectively.

Neighbor instability was higher in larger (30 and 50 individuals) than in smaller flocks (10 individuals) ($Q_4(3s)$; $p-value < 0.001$, ANOVA) for both roosting and evasive turns ($p-value = 0.7$, ANOVA) (Figure 4.4) and when interacting with a larger number of nearby neighbors (increased topological range, $p-value < 0.001$; Figure 4.5A). This increase may be a side-effect of increased density when interacting with more neighbors: the smaller distance between flock members may force them to turn more to avoid collisions and thus change their relative positions faster.

Another characteristic linked to increased predation pressure is the increased reaction frequency of individuals [79, 41]. In our model, higher reaction fre-

quency (interacting more often with nearest neighbors) leads to higher instability of neighbors (Figure 4.5B), because individuals re-adjust their position to each other more often and are thus turning more.

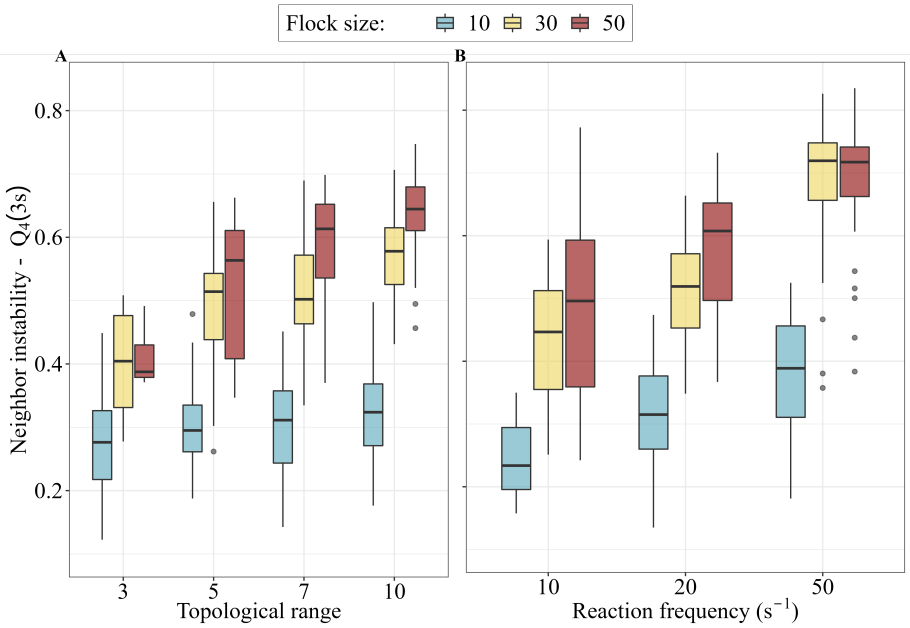

Figure 4.5: **Coordination specifics.** The effect of topological range (A) and reaction frequency (B) on the instability of neighbors after 3 seconds of turning in flocks of 10, 30 and 50 individuals, in both evasive and roosting turns.

Concerning their interaction rules, the higher the tendency of flock members to align, the more stable their neighborhood remained during roosting turns (ANOVA; $F-value = 26.75$, $p-value < 0.001$; S4.1 Figure). In evasive turns, there was no effect of alignment tendency on the instability of neighbors (ANOVA; $p-value = 0.65$). This difference may emerge from a higher occurrence of collision avoidance during roosting, since differences among-individuals in their turning tendencies are larger. Alignment may act as an alternative mechanism for collision avoidance (individuals with parallel headings will never collide) and thus smooth out the reshuffling of individuals due to differences in their local conditions (their relative position to the roost). According to our initial hypothesis, centroid attraction has the opposite effect, its increase led to higher instability of neighbors, for both roosting (ANOVA; $F-value = 20.6$, $p-value < 0.001$) and evasive turns (ANOVA; $F-value = 12.3$, $p-value < 0.001$) (S4.1 Figure).

In sum, the highest instability of neighbors is found in large flocks with high number of topological neighbors and strong centroid-attraction ($Q_4(3s) \approx 0.8$)

and the lowest instability ($Q4(3s) \approx 0.1$) in small flocks with few interacting neighbors and strong alignment.

4.4.2 Instability and turning modes

The deviations from turns with equal-radii and parallel-paths were smaller for individuals closer to each other (increased deviation with increasing neighbor rank, Figure 4.6). The deviation from parallel-paths increased exponentially with time (Figure 4.6A), while from equal-radii it reached a plateau (resembling a sigmoid function, Figure 4.6B). For the rest of our analysis, we focused only on the deviation of the nearest neighbor at the end of our 3 seconds sliding window. Across our simulations, the collective turn that was closer to a turn with parallel-paths was one of a small flock (10 individuals) roosting with low turning rate ($D_p(3s) = 0.14$ m).

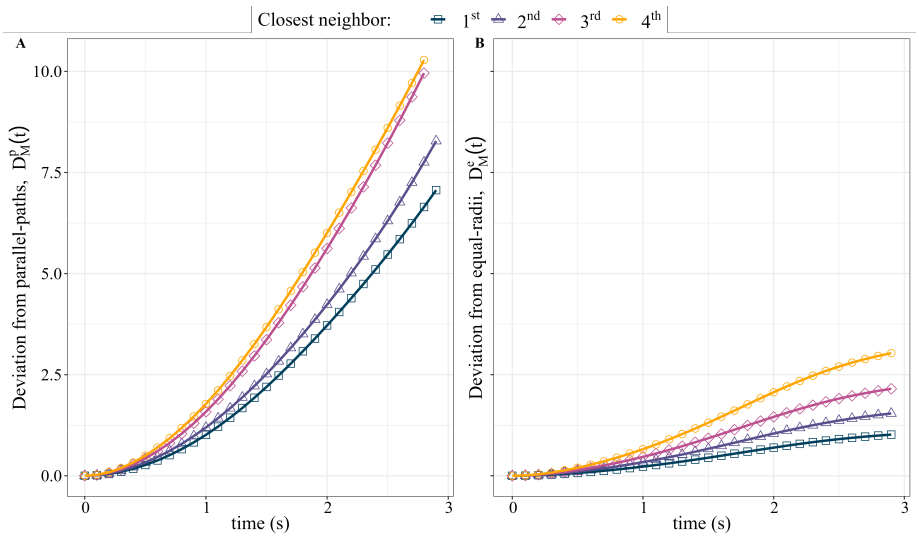

Figure 4.6: **Average deviation from the two turning modes** (A) parallel-paths (D^p) and (B) equal-radii (D^e), during collective turns based on the 4 closest neighbors. The deviation is lower the lower the neighbor's rank (1^{st} closest vs 4^{th} closest).

We expected the instability of neighbors to increase with decreasing deviation from turns with equal-radii and to decrease with decreasing deviation from parallel-paths (since during a turn with parallel-paths individuals keep their relative positions stable and neighbor instability is expected to be 0). However, the relation between neighbor instability and deviation from the two turning modes was not linear. Overall, we found weak positive correlations between instability of neighbors and deviations from parallel-paths (Spearman correlation; $R = 0.58$, $p-value < 0.001$, S4.2 Figure; according to our H7 hypothesis)

and equal-radii (Spearman correlation; $R = 0.55$, $p-value < 0.001$, S4.2 Figure; opposite to our H6 hypothesis). Unexpectedly, deviation from equal-radii also positively correlated with deviation from parallel-paths (Spearman correlation; $R = 0.7$, $p-value < 0.001$, S4.2 Figure). However, across our parameter space, the relation between the three measurements (neighbor instability and deviations from parallel-paths and equal-radii) varied according to the varying parameter, with no correlation between them across smaller changes in parameter values (for example across simulations with evasive turns in which only flock size changes; Qm-De: $R = 0.04$, $p-value = 0.64$; Dp-De: $R = 0.25$, $p-value = 0.004$).

We often saw counter-intuitive changes in deviations and neighbor instability; we summarized all effects in Figure 4.7. For instance, during roosting turns, increased topological range led to lower deviation from turns with both parallel-paths (GLM; $t-value$ = -11.8, $p-value < 0.001$) and equal-radii (GLM; $t-value$ = – 21.9, $p-value < 0.001$), while neighbor instability slightly increased (GLM; $t-value = 7.5$, $p-value < 0.001$) (S4.3 Figure).

Larger flocks showed larger deviation from turns with both parallel-paths (ANOVA, evasive turns: $F-value = 9.4$, $p-value = 0.003$; roosting turns: $F-value = 85.9$, $p-value < 0.001$) and equal-radii (but only during roosting, ANOVA, evasive turns: $p-value = 0.06$; roosting turns: $F-value = 16.6$, $p-value < 0.001$) (Figure 4.7). Increasing the reaction frequency of individuals showed the expected effect in roosting turns (according to our findings on neighbor instability): it decreased the deviation from equal-radii ($F-value = 344$, $p-value < 0.001$) and increased the deviation from parallel-paths ($F-value = 319$, $p-value < 0.001$). Interestingly, in evasive turns we saw the reverse effect on the deviation from equal-radii ($F-value = 31.4$, $p-value < 0.001$). In total, measurements of evasive turns seemed to be more robust against changes in our parameters (Figure 4.7); this highlights the importance of small difference in the tendency to turn (turning rate) among flock members.

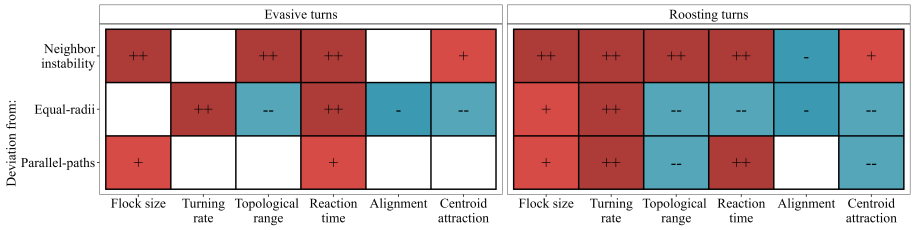

Figure 4.7: **The effect of our parameters on neighbor instability, deviation from equal-radii and parallel-paths.** The colored tiles show positive (in red, with + labels) or negative (in blue, with – labels) relation between a parameter and a measurement, and the signs represent strong (++, – –) or weak (+, –) effects. Empty tiles represent non-significant effects ($p-values > 0.05$).

4.5 Discussion

We examined the link between the specifics of coordination of flock members and neighbor instability during collective turns, using instability as a proxy of predator confusion. We did so in our new computational model of collective turning. In it, collective turns are initiated by one or a few flock members, similar to empirical data [115]. To study the relationship between neighbor instability and the two modes of collective turning (equal-radii and parallel-paths [142]), we developed a metric of deviation from these modes. In our simulations, we find many counter-intuitive effects between parameters and our measurements.

Instability of neighbors (measured after 3 seconds of turning) varied across our simulations, covering the instability measured in real flocks [27]. Higher instability of neighbors emerged in a previous computational model from a decrease in the topological range of collision avoidance (when individuals avoid a single neighbor instead of their closest 7 neighbors) [72]. In our simulations, it emerges from an increase in the topological range of alignment and centroid attraction (when individuals interact with a higher number of neighbors). Thus, interacting with many neighbors may have a strong anti-predator effect, not only through increased speed of information transfer through the flock [115], but also by increasing the predator's confusion. This relation between topological range and neighbor instability may further explain why reduced topological range is found in other ecological contexts where keeping a stable neighborhood is favorable (for instance in jackdaws flying with their mating pair [112]).

Other parameters that lead to higher instability of neighbors in our simulations are larger flock sizes, stronger centroid-attraction, and higher reaction frequencies. Neighbor instability increases less between flock sizes of 30 and 50 individuals than 10 and 30 individuals. Since this effect may depend on the local volume of the group, it remains to be studied whether there is a critical point after which further increase in flock size does not affect neighbor instability. Stronger centroid-attraction increases the density of a group. In a denser flock with metric interactions among flock members, the number of interacting neighbors is expected to increase. Thus, we predict that a switch from topological to metric interactions in flocks of high density, as found in jackdaws during mobbing flights [114], will increase the confusion of the predator. Furthermore, increased reaction frequency has been identified in groups under predation [41, 79]. According to our model, such an increase in reaction frequency will also confuse the predator through increased instability of neighbors.

In a collective turn with parallel-paths, neighbor instability is 0 (no neighbor is changing); we thus expected the parameters that led to high neighbor instability to also lead to high deviation from parallel paths. Surprisingly, many of our coordination parameters showed the opposite: roosting turns with in-

creased topological range and stronger centroid-attraction deviated less from parallel-paths despite their higher instability of neighbors. This may be a side-effect of increased collision avoidance and coordination by averaging over more neighbors: individuals may lose the neighbors that are furthest away more often (and thus increase their neighbor instability), but keep their closest neighbor in a more stable relative position (decreasing the deviation from parallel-paths). These self-organized processes highlight that the relationship between flocking properties (such as neighbor instability) and turning modes is more complex than we previously assumed.

Whether the formation and internal structure of a flock during a turn has adaptive value is unclear. Turning with parallel-paths has been ruled out as a plausible behavior of bird flocks since it is assumed to require more energy (individuals need to adjust their speed) and to not confuse the predator like turns of equal-radii [10, 8]. Thus, turns of equal-radii were assumed to be a better escape strategy and the extreme opposite of parallel-paths turns [10, 185]. Our results challenge these hypotheses; the deviations from parallel-paths and equal-radii often positively correlated and both showed positive and negative correlations with instability of neighbors. In addition, turns closer to parallel-paths may be favorable if the relative position of group members itself is energetically advantageous (for instance during V-formations [28]) or social-bonds in the group make it important for individuals to keep the same neighbors (for instance when flying with mating partners [112]).

A challenge when studying collective turns is the interconnection of many emergent factors concerning a flock's characteristics (internal structure, flock shape, and turning mode). Disentangling the indirect effects of parameters on the dynamics of each turn is not straight forward; a parameter may alter the shape or density of the flock, which can affect other flock characteristics during a collective turn. To understand this interconnection, more insight is needed in the relation between flock shape, diffusion and turning mode. Our new model and metric of deviation from the two turning modes provide a framework in which this can be studied, with our metric being the first to quantitatively capture the resemblance of a collective turn to the two turning modes. One potential limitation of our model is its 2D representation. Even though flocks are not expected to change altitude during a collective turn [27, 185], the crossing of individual paths during a turn may cause the collision avoidance in our model to have a disproportionately large effect on the type of collective turn (larger than it would have in a 3D simulation).

Understanding collective turning can not only provide the theoretical insight discussed above, but also aid the development of future models and enable biomimetic applications of collective motion. First, neighbor instability, internal structure and flock shape are emergent characteristics of a flock that can be used to examine the resemblance of a model to reality [115]. Thus, a better

understanding of how flock characteristics change across the parameter space may facilitate the tuning of new models to empirical data, supporting their validation across several patterns [59]. Secondly, improved information transfer through neighbors' reshuffling (instability) in a group is of great importance for many systems of swarm robotics [1, 180]; thus, a deeper understanding on which individual rules lead to high instability of neighbors is valuable [100, 187]. On the contrary, when the goal is to keep the relative position of individuals constant (formation flight) and avoid collisions (for instance for the development of self-organized swarms of drones) [178, 187], our parameter combinations that lead to low deviation from parallel-paths may be beneficial.

4.A Supporting information

Supplementary Figures

S4.1 Figure. Instability of neighbors with increasing strength of alignment and centroid attraction for both roosting and evasive turns in flocks of 30 individuals.

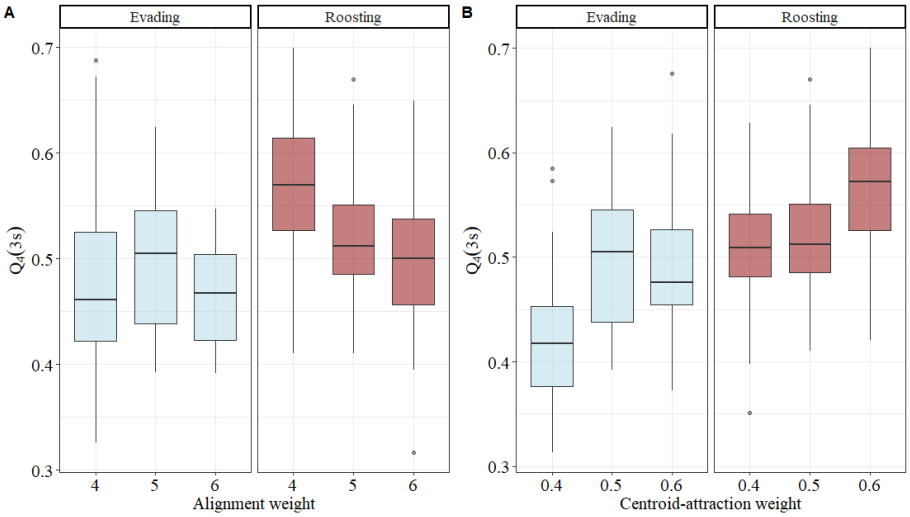

S4.2 Figure. Correlation between instability of neighbors, deviation from parallel-paths and equal-radii, in flocks of 10 to 50 individuals during evasive and roosting turns of varying size.

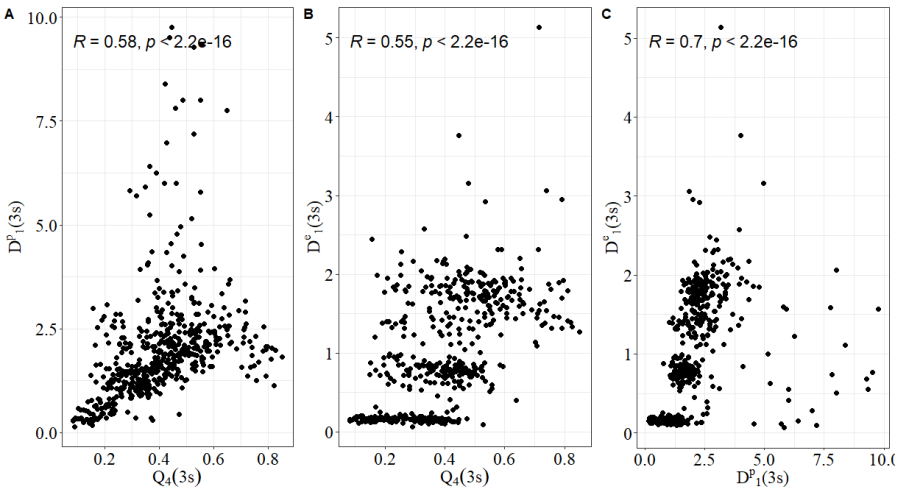

S4.3 Figure. The effect of topological range on deviations from parallel-paths (A), equal-radii (B) and instability of neighbors (C) in roosting turns across all flock sizes.